Proceedings of PVP2005
2005 ASME Pressure Vessels and Piping Division Conference
July 17-21, 2005, Denver, Colorado USA

PVP2005-71322

INTRODUCTION OF THE ELEMENT INTERACTION TECHNIQUE FOR WELDING ANALYSIS AND SIMULATION

Ihab F. Z. Fanous
Faculty of Engineering & Applied Science
Memorial University of Newfoundland
St. John's, NL, Canada
fanous@aucegypt.edu

Dr. Maher Y. A. Younan
Professor of Mechanics and Design
Mechanical Engineering Department
The American University in Cairo, Egypt
myounan@aucegypt.edu
Tel: (202) 797-5336, Fax: (202) 795-7565
(contact author)

Dr. Abdalla S. Wifi
Professor
Mechanical Design and Production Department
Cairo University, Egypt
aswifi@aucegypt.edu

ABSTRACT

The residual stresses generated due to welding in pressure components may have several harmful effects such as decrease in the resistance to cycling load and corrosive environments. The analysis of the welding process has been developed extensively in 2D and 3D. The element movement technique has been shown to be very effective in simulating the filler material deposition leading to a reduction in the analysis time. However, when attempted for wider fields of applications, it had some limitations, especially when moving the elements towards the base-plate.

In this paper, the element interaction technique is introduced utilizing the concepts of both the element movement and element birth techniques. The new technique is verified versus the currently developed procedures. In this technique, the elements of the weld pool are held in place in contact with the elements of the base-plate and the interaction is made to be a function of time. This gave several flexibilities in modeling the welding process. Hence, the technique is then used to analyze simple fillet welding of a plate and circumferential butt-welding of a pipe.

INTRODUCTION

The residual stresses generated during welding vary with the change in the welding parameters depending on the procedure of the joining process. Many researches have been done to investigate the residual stress for specific problem. Due to the complexity of the different applications, several assumptions and approximations, such as reducing the model from 3D to 2D, are made to facilitate the analysis. These approximations help mainly in reducing modeling efforts and analysis time.

The element birth technique has been used in simulating metal deposition in both 3D and 2D models. Brown and Song [1] have used the technique in an axisymmetric simulation of a fillet-weld of ring-stiffened cylinder. Wilkening and Snow [2] have also solved an axisymmetric simulation of a two-pass butt-weld of a cylinder using the element birth technique. Also, for a plate, they assumed that the through thickness variation of the residual stress is insignificant, so they modeled a single-pass butt-weld of plate using 2D plane model of the plate. Bouchard et al [3] has also used the element birth technique for axisymmetric model of a 23-pass weld of a nozzle. Dong [4] has developed both an axisymmetric model and a 3D shell model for a circumferential butt-welding of a pipe. He used the results of the former to interpret that of the latter. Goldak [5] made one of the early studies in the advantages of a full 3D model of the welding process. He compared the different forms of 2D approximation to full 3D analysis of the welding process. A common comment among all the previous work that any discrepancy in the results is mainly due to the approximation of the modeling from a full 3D to different forms of 2D

In modeling the welding process using the element movement technique developed in [6] and [7], several draw-backs were discovered when simulating a fillet weld. In modeling the element movement technique, gap elements were introduced between the nodes of the weld pool and the nodes of the base plate. These gap elements were responsible for the thermal interaction between the two bodies. For the structural interaction, a constraint equation is activated at the moment the nodes of the weld pool reach the nodes of the base plate. This constraint equation couples the degrees of freedom of the nodes getting into contact. When applying this procedure to the fillet weld, the finite element code ABAQUS [8] did not accept the inclined symmetry boundary condition along with the coupling with the base plate for the nodes at the lowest point of the weld pool.

In addition, another problem came up in modeling the fillet welding process using the element movement technique which is the meshing of the weld pool. Meshing a triangular cross section or any other shape that cannot be divided into regular eight-nodded brick elements requires a huge effort in arranging the nodes of the weld pool so as to create slices that would move one after the other towards the base plate. Managing the node numbering in order to minimize such effort for the above weld pool is a cumbersome task whether it is done manually or using any pre-processor. Hence, it was essential to introduce another procedure that would be independent on the elements arrangement. This can be achieved using surface-to-surface interaction instead of node-to-node interaction.

In this paper, element interaction technique is introduced to facilitate the analysis of different welding processes and also reduce the analysis time. The three models developed in [9] are remodeled

using the new element interaction procedure for verification. These models simulate the butt-welding of a plate subjected to different boundary conditions. The procedure is then used to analyze two different applications which are the fillet-welding of a plate and circumferential butt-welding of pipe for different structural boundary conditions. For the fillet-weld model, a study is made to check for the effect of the welding parameters on the generated residual stresses. The welding parameters that are studied are the total heat input and the welding speed.

FINITE ELEMENT MODELS

A verification model (Model 1) simulating the butt welding of two plates is developed which is similar to that used in [7] and [9]. In addition, two other models are developed simulating fillet welding (Model 2) of a plate and circumferential butt-welding of a pipe (Model 3). In the first model, the three boundary condition sets shown in [9] are applied as well as the moving heat source, using the user-defined subroutines, temperature dependant materials properties and filler material deposition utilizing the element interaction technique. These models are analyzed using ABAQUS Standard commercial code.

Butt-Welding of a Plate (Model 1)

The model simulates basic arc welding of two coplanar plates along the parting line with the addition of a filler material between them as illustrated in Fig. 1. The model is developed similar to that shown in [7] and [9].

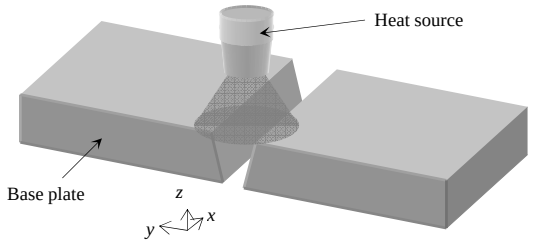

Figure 1: The diagram of the welding process

Each plate has a length of 100 mm (x-direction), width of 50 mm (y-direction) and height of 5 mm (z-direction). The welding speed is 1 mm/s. Parametric meshing is used in order to easily track the results along a certain predefined path in any direction as shown in Fig. 2(a). The element used is an 8-node brick element that can perform a coupled displacement-temperature analysis. In order to implement the element interaction technique, the elements of the base plate are not directly joined to those of the weld pool. However, the two parts shall remain in direct contact as opposed to the element movement technique where the elements of the weld pool are shifted slightly in the z-direction. The interaction between the two bodies is governed by surface-to-surface thermal and structural contact between the two shaded surfaces indicated in Fig. 2(b).

The user-subroutine UNITER is developed to define the behavior of the surface-to-surface interaction between the two bodies. It includes both the structural and thermal interactions. As explained in [7] and [9], the key issue in the element movement technique is the gradual increase in the conductance between the two bodies in order to avoid the occurrence of a sudden high temperature gradient. Hence, in the UINTER subroutine, the conductance between the surfaces is set to be a function of time. Figure 3 shows a plot of the conductance versus the position along the welding line. In order to simulate the deposition of molten metal, the nodes of the weld will have an initial temperature above the liquidous level.

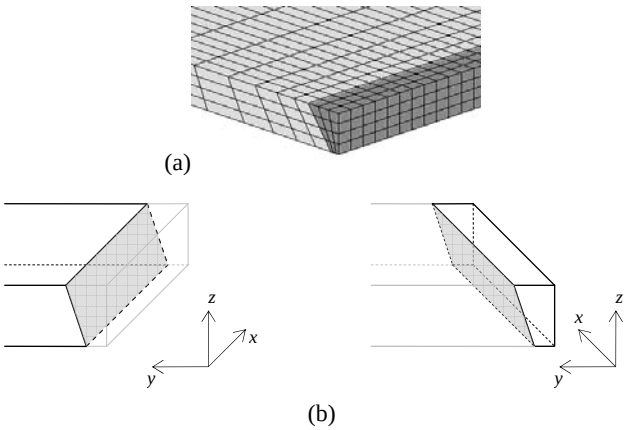

Figure 2: (a) Meshing of the plate and the weld pool. (b) A schematic diagram of the contact surfaces

Before welding starts, all the contact points will be in Zone A where the conductivity is set to zero. As the heat source moves along the welding line, the contact points start to get into Zone B where the conductivity starts to increase gradually from zero at a very small slope. The purpose of the gradual increase in the slope of the curve is avoiding a sudden huge amount of heat flow when the conductivity starts to increase. Hence, to have both a gradual decrease in the difference in temperature and also a gradual change in the amount of heat flowing between the two bodies due their difference in temperature, a parabolic curve of the conductivity is required. The conductivity reaches the maximum level at the center of the heat source. The contact points which the heat source has already passed by will be in Zone C where the conductivity remains at the maximum level maintaining the difference in temperature between the two bodies near zero.

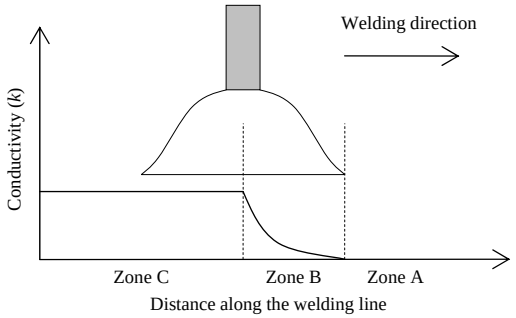

Figure 3: Diagram of the variation of gap conductivity

As for the structural interaction, a large attraction force is introduced between the two surfaces. Hence, if the gap distance increase due to deformation of the two bodies, the attraction force will decrease it to the minimum value possible. It was noticed that, if the gap distance is small, a large force would cause some unpredictable large distortions in the elements of the weld pool where the temperature is above the liquidous level and, thus, leads to divergence in the analysis. Hence, the attraction is set to be proportional to the gap distance at every point of contact between the two surfaces. This is done by using the gap distance, being passed as a parameter to the UINTER subroutine, and calculating the force

accordingly. Since the estimated gap distance depends on the time increment during the analysis, any convergence problems occurring due to the attraction force will be handled by the time increment as well. Hence, when the gap distance increases, the force will be large and after several iterations within every increment in the analysis they both converge to small values. Having the elements of the weld pool in continuous contact with those of the base plate through the attraction force will have an insignificant effect on the stress distribution. This is because the nodes of the weld pool are set to have an initial temperature beyond the liquidous level which makes the elements very soft in comparison to those of the base plate.

The three boundary conditions sets demonstrated in [7] and [9] are considered in order to verify the element interaction technique. In the first set, the plates are clamped at one end and welded along the joining side, as shown in Fig. 1, after which the plates are released and checked for residual stresses. In the second boundary conditions set, the plates to be welded are simulated to be part of a large structure so that the plate may expand freely but with no rotation allowed even after the welding process is finished. The same thermal load is applied in both set 1 and set 2. In the third set, the structural boundary conditions are the same as that of set 1 but with a decrease in the thermal load.

Since the welding process is applied along a straight line, only one plate shall be modeled applying symmetry boundary conditions to it. For thermal symmetry, the heat flux passing across the surface of symmetry shown in Fig. 4 is set to be zero, and, for structural symmetry, the translation in the y-direction of the same surface is also zero.

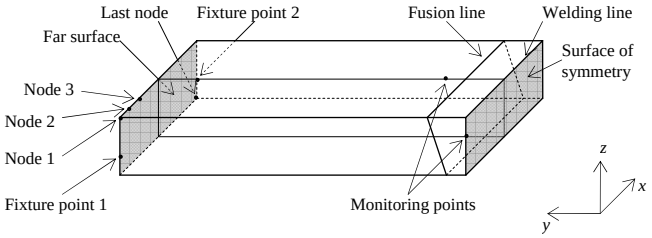

Figure 4: Major points, paths and surfaces in Model 1

When considering the structural boundary conditions, in boundary condition set 1, the far surface shown in Fig 4 is constrained in the y-direction throughout the whole welding process and then released after complete cool down to check for the residual stress at no load. For structural stability, fixture point 1 is constrained in the x and z directions, and fixture point 2 is constrained in the z direction after the complete constraint of the far surface is released. Although this might affect the shape of the weld pool cavity before metal deposition since the base plate is free to expand towards the weld pool (y-direction), the newly activated elements take the new shape since they share common nodes with the base plate. In boundary conditions set 2, slight movement of the far surface in Fig. 4 is allowed but with no rotation about any axis which is simulated by forcing the y-displacements of all the nodes on the far surface to be the same. This is modeled by using a constraint equation that couples the y-component of the displacement of each two consecutive nodes on the surface. Therefore, with reference to Fig. 4, the y-displacement of node 1 is set to be equal to that of node 2 and that of node 2 is set to be equal node 3, etc… This way y-displacement of the all the nodes would be equal starting from node 1 to the last node on the surface. Finally, in boundary condition set 3, the structural boundary conditions are similar to those of set 1. However, the thermal load is changed by altering the total heat input from 1300 to 900 watts.

The moving heat load is applied as distributed heat flux to the top surface of the model. The region within which the heat is applied has a circular shape assuming the heat source is applied perpendicular to the plate without any inclination. The user-subroutines named DFLUX and FILM developed in [7] and [9] using the FORTRAN language are used to apply the thermal load of the moving heat source and the thermal boundary conditions that vary according to the moving heat source, respectively, to the top surface of the plates. The thermal boundary conditions include the radiation and convection to the environment from all sides of the welded plate except the symmetry surface and the area upon which the heat is applied.

The analysis of this model is conducted in two steps for boundary condition set 1 and 3. One is the welding process itself including the cooling down time, and the other is where the fixation of the far surface is released. The analysis for boundary condition set 2 is done in only one step as the boundary conditions do not change. It can be noted that there is huge simplification in the modeling procedure of the welding process using the element interaction technique in comparison to earlier methods where a step is defined for every group of elements either being activated (the element birth technique) or moved (the element movement technique).

Fillet-Welding of a Plate (Model 2)

This model simulates the fillet welding process of two plates joined at 90°. Figure 5 shows a schematic of the process. Each plate is 100 mm (z-direction) by 50 mm (x-direction) and 5 mm thick (y-direction). The welding speed is set at different values. For every welding speed, the residual stresses are checked for different heat input power.

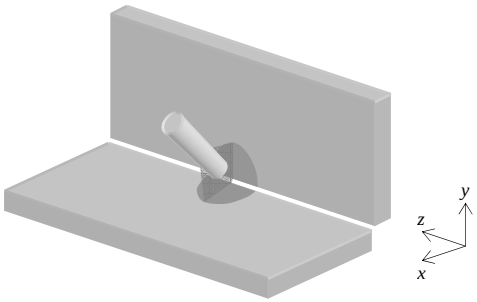

Figure 5: Schematic diagram of the fillet-welding process

The model shall be tested for welding speeds of 1.0, 1.5, 2.0, 2.5 and 3.0 mm/s and different heat inputs. In selecting the heat power input, it should be noted that sufficient heat must be applied to increase the temperature of the base plate at the position of the heat source to a level beyond the liquidous level. Therefore, the minimum heat input for the low speed will be lower than that of the high speed. The minimum heat input for the above mentioned speeds will be 1800, 2200, 2500, 2800 and 3100 watts, respectively.

The interaction between the two bodies is modeled in the same manner as Model 1. Figure 6 shows the surfaces of the bodies being assigned to have both structural and thermal interaction.

In this model, the plates are constrained in way to avoid rigid body motion. This is achieved by setting point 1 shown in Fig. 7 to be constrained in the x and z directions, and point 2 constrained in the x-direction. In addition, the surface of symmetry will be constrained in

direction normal to the surface accounting for the symmetry of the structure.

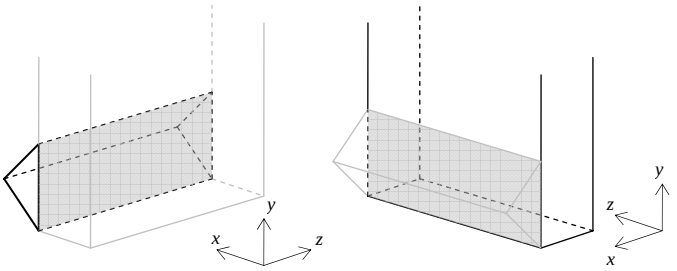

Figure 6: Contact surfaces in Model 2

The heat source is modeled by applying a surface heat flux to the top surface of the weld pool indicated in Fig. 7. The heat flux is applied in a circular area with a normal distribution as described in [9]. The plane of the heat flux circle is parallel to that of the top surface of the weld pool and its center point would move along the welding line. Similarly, heat would be lost through convection and radiation from area around the circle of the heat source except for the part of the top surface of the weld pool that is ahead of the heat source as explained in [9]. The moving heat source and loss are modeled using the DFLUX and FILM user subroutines, respectively, that are used in Model 1. In addition, heat is lost from all sides of the plate through convection and radiation except those surfaces that are in contact. For symmetry, the surface of symmetry indicated in Fig. 7 will have a heat flux of zero.

The analysis of the model is done in a single step as opposed to Model 1 as the boundary conditions do not change.

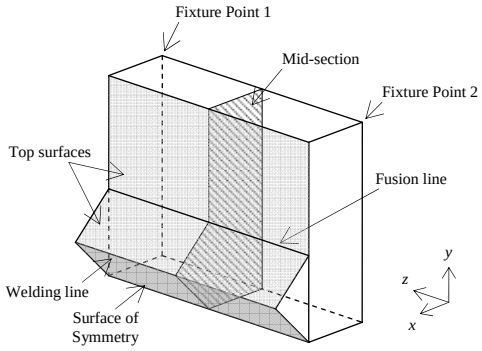

Figure 7: Major points and paths of Model 2

Circumferential Butt-Welding of a Cylinder (Model 3)

The modeling of the element interaction has a great flexibility when it comes to different welding paths. The following model simulates the circumferential butt-welding of a cylinder. The inside diameter of the cylinder is 60 mm and the thickness is 5 mm. The welding speed is set to 1 mm/s. The minimum heat input found to be suitable with this speed is 1500 watts. Figure 8 shows a schematic diagram of the model.

To model the element interaction technique, the weld pool and the base cylinder are modeled as separate parts. The interaction between the two parts is modeled using surface-to-surface interaction. It can be noted that the difference in the welding path from Model 1 is that the starting point is the same as the ending point. This required the introduction of an interaction between the two surfaces that are at the start and end of the weld pool. This interaction would be inactive at the beginning of the welding process and activated near the end of the process.

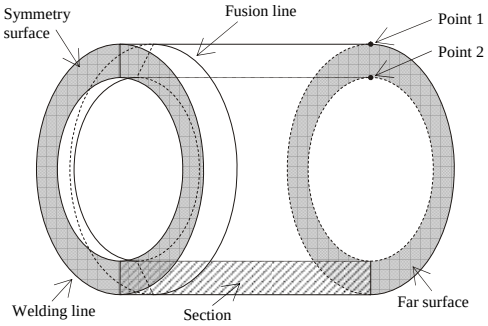

Figure 8: Schematic diagram of Model 3

The user-subroutine UINTER that was developed earlier in Model 1 is modified to include the interaction between the start and the end surfaces illustrated in Fig. 9. Also, the start surface is set to loose heat during the welding process through heat convection and radiation, and gradually stops the heat lost as the heat source approaches the end point. This is done by setting the coefficients of the heat loss varying with time so that they would be at the maximum value during the welding process and gradually decreases to zero when the start point becomes in the region of the heat source.

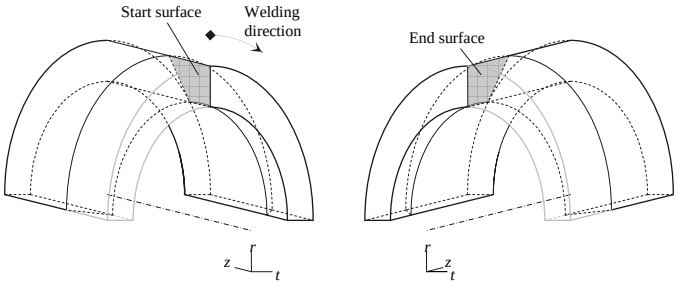

Figure 9: Start and end points of the welding path

Parametric meshing is performed using 8-node solid brick element for coupled displacement-temperature analysis. The model is analyzed using 2 boundary conditions similar to sets 1 and 2 of Model 1. In set 1, the far surface shown in Fig. 8 is fixed and then released after complete cool down. In boundary condition set 2, nodes of the far surface are coupled in a way such that their axial displacement will be equal. This simulates the cylinder being a part of a long pipe. The total heat input in both models will be 1500 watts.

Material Properties

The material properties in this study are acquired from Brown and Song [1] having properties shown in Table 1. The latent heat indicated is included by ABAQUS in the specific heat variation with temperature between the liquidous and solidous levels.

Table 1: Material properties versus temperature

Temperature (ºC)	20	1550	1650	2000
Young's modulus (GPa)	200	0.2	2×10^{-5}	2×10^{-5}
Poisson ratio	0.25	0.25	0.25	0.25
Yield strength (MPa)	290	1	0.01	0.01
Yield strength at strain 1.0 (MPa)	314	1	0.01	0.01
Thermal expansion ($1/ºC \times 10^{-6}$)	10	15	15	15
Thermal conductivity (W/m·ºC)	50	30	30	30

Specific heat (J/kg·ºC)	450	400	400	400
Latent heat (J/kg)	260000			

RESULTS AND DISCUSSION

Verification model (Model 1)

The element interaction technique showed to be very effective in modeling the metal deposition of the welding process. Figure 10 and 11 shows the comparison between the temperature histories using both techniques. A good match can be observed in the thermal response.

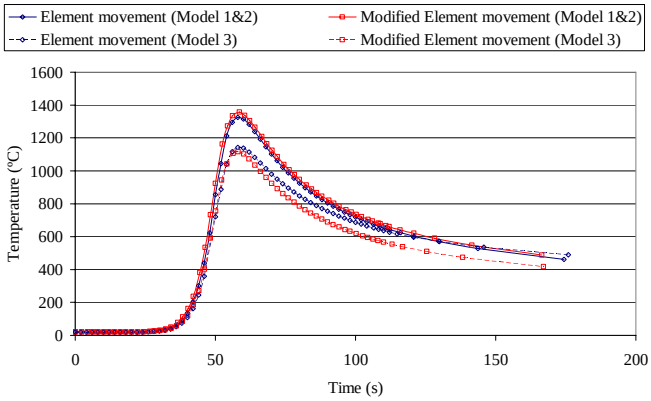

Figure 10: Temperature history at the top monitoring point using element movement and element interaction techniques

Figure 12 shows a comparison of the residual stresses along the welding line and the mid-section for boundary condition set 1 and 2. A close match between the two sets of results can be observed. Some discrepancies may be noticed due to the difference in the numerical models.

Fillet-weld (Model 2)

The results of the fillet weld had the same trend as that of the butt weld. The residual stresses generated due to the change in the heat source were quite negligible, while the effects of the change in the boundary conditions were large. Figures 13(a) and (b) show a comparison of the stress distribution along the welding and fusion lines, respectively, in Model 2 for different values of the heat input for boundary condition set 1 while fixing the other welding parameters. It can be noticed that the heat input has a minor effect on the residual stresses which was the case in the butt-welding shown in Model 1. This can also be observed from Fig. 13(c) and (d) comparing the stress distribution along the top and bottom of the mid-section, respectively. The same effect for the change in the heat was observed for boundary condition set 2.

The model was also analyzed for 5 different speeds for both the free and coupled structural boundary conditions. The same effect was also observed for different welding speeds. However, changing the welding speed caused some variation in the residual stress distribution, especially along the bottom side of the plate. Figure 14(a) shows that there is an increase in the longitudinal stress near the ends of the welding path tending to go closer to that near the mid point, accompanied by a decrease in the transverse stress near the middle. It can be also observed that the increase in speed changes the variation of the stress distribution along the path. Since the fillet weld heats up only one side of the plate, it would be expected to have some variation in the residual stresses from top to the bottom side of the plate. Figure 14(b) illustrates that the bottom side of the plate is highly affected by the change in the welding speed. This is because, at high speeds, the temperature at the bottom side does not reach a high level as low speed. Hence, the longitudinal stress decreases at the bottom side of the plate as the welding speed increases. The variations in the stress distribution along the welding line are accompanied by some variation within the plate away from the welding line. This is illustrated in Figs. 14(c) and (d).

Circumferential Butt-welding of a cylinder (Model 3)

The residual stresses generated in the cylinder have different distribution trends than that in plates shown in Model 1 and 2. The thermal expansion and contraction taking place along the welding line causes some bending stresses in the axial direction. This is illustrated in Fig. 15(a) which shows the distribution of the residual radial, hoop and axial stresses along the welding line at the outer and inner surfaces. It can be observed that there is a change in the axial stress from positive at the outer surface to negative at the inner surface of the cylinder. Another effect of the circular path (the end point is the same as the start point) is that the residual hoop and axial stresses drop to a high compressive value at a short distance from the start point with a very high gradient. The radial stress is very small compared to the other components. Figures 15(b) and (c) show the decay of the stresses in the axial direction at angles 90° and 270° from the starting point. All the components tend to stabilize at the distance from the welding line.

The stresses in the boundary condition set 2 with coupled far surface increased similar to the case in Model 1 of the plate. This is shown in Fig. 15(d). Also, the decay of the stresses in the axial direction, shown in Figs. 15(e) and (f), is similar to that of boundary condition set 1 except that the axial stresses stabilize to a value different than zero. Hence, since boundary condition set 2 simulates the cylinder being part of a long pipe, the residual stresses at the far surface represents the residual stress in a long pipe.

CONCLUSION

In comparing the element interaction technique versus the element movement technique developed earlier, it can be observed that the former showed to be very effective. It allowed modeling of wider range of applications in simpler steps. Also, the stress history and the residual stress distribution resulting from both techniques compared well, with an acceptable difference.

Welding speed in the fillet welding process has a great effect on the distribution of the generated residual stresses, as opposed to the thermal load which hardly affects the level of residual stresses. Selection of the appropriate welding speed would depend on the nature of loading that will be applied to the component after the joining process. Welding a free plate caused a much lower residual stresses than welding a plate that is part of a larger structure. The same effect of the change in boundary conditions is observed in welding a cylinder.

REFERENCES

[1] Brown, S., and H. Song, 1992, “Finite Element Simulation of Welding Large Structures,” Journal of Engineering and Industry, **114**, pp. 441-451.

[2] Wilkening, W. W. and J. L. Snow, 1993, “Analysis of Welding-Induced Residual Stresses With The Adina System,” Computers and Structures, **47**, No. 4/5, pp. 767-786.

[3] Bouchard, J., P. Holt and D. Smith, 1997, "Prediction and Measurement of Residual Stresses in a Thick Section Stainless Steel Weld," ASME PVP, Vol. 347, pp. 77-82.1.
[4] Dong, P., May 2001, "Residual Stress Analyses Multi-Pass Birth Weld: 3-D Special Shell versus Axisymmetric Models," Journal of Pressure Vessel Technology, **123**, pp. 207-213
[5] Goldak, John, 1990, "Keynote Address: Modeling Thermal Stresses and Distortions in Welds," Recent trends in welding science and technology, ASM International, Ohio
[6] Fanous, Ihab F. Z., February 2001, "3D Modeling of the Welding Process Using Finite Elements," M.Sc. thesis, The American University in Cairo, Egypt
[7] Fanous, Ihab F. Z., Maher Y. A. Younan, Abdalla S. Wifi, 2003, "3D Modeling of the Welding Process Using Finite Elements Using Element Birth and Element Movement techniques," Journal of Pressure Vessel Technology, **125**, pp. 144-150.
[8] Hibbitt, Karlsson and Sorensen, 2003, "ABAQUS/Standard User's Manual."
[9] Fanous, Ihab F. Z., Maher Y. A. Younan, and Abdalla S. Wifi, 2003, "Study of the Effect of Boundary Conditions on Residual Stresses in Welding Using Element Birth and Element Movement Techniques", Journal of Pressure Vessel Technology, **125**, pp. 432-439

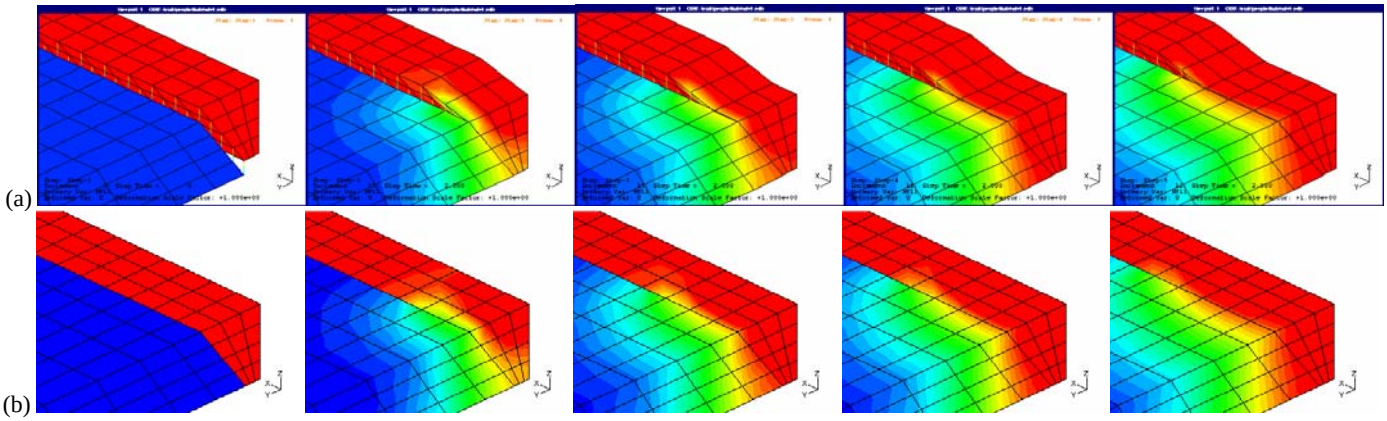

Figure 11: Comparison between the heat flow in the (a) element movement technique and the (b) element interaction technique

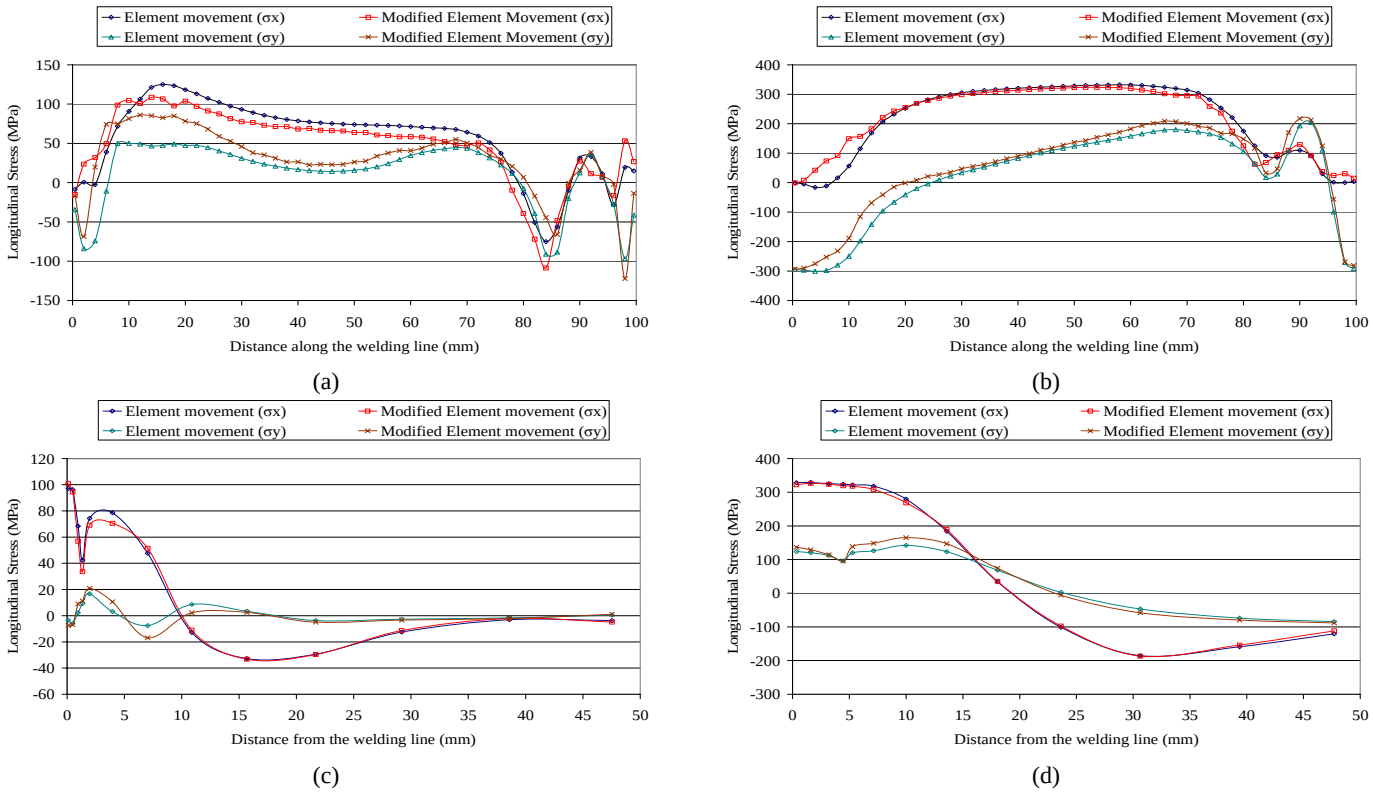

Figure 12: Comparison of the longitudinal and transverse residual stress along the welding line for (a) boundary conditions set 1 and (b) boundary conditions set 2, and top of mid-section for (c) boundary conditions set 1 and (d) boundary conditions set 2 between the element movement and element interaction techniques

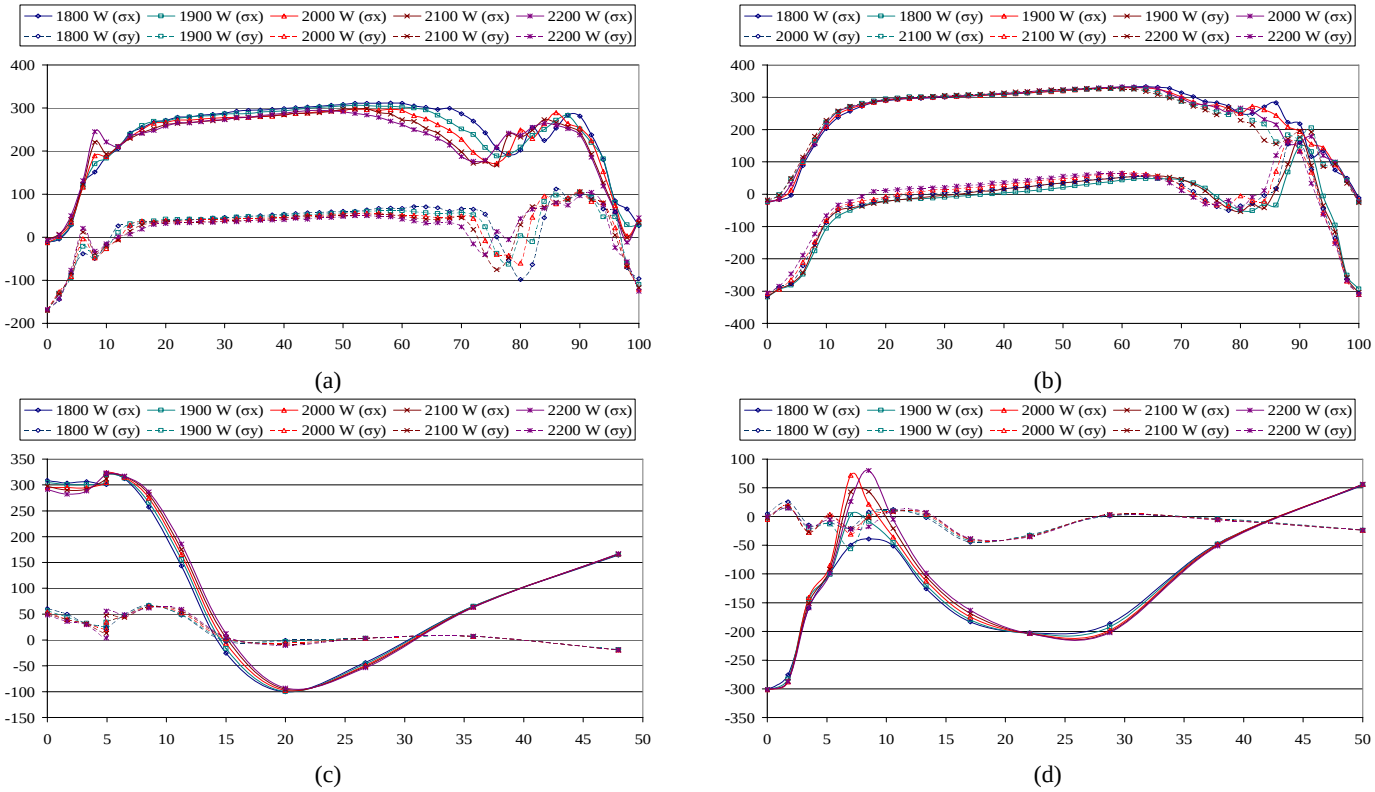

Figure 13: Residual stress distribution of Model 2 boundary condition set 1 (a) along the top of the welding line, (b) the bottom of the welding line, (c) top of the mid-section and (d) bottom of the mid-section for different heat inputs

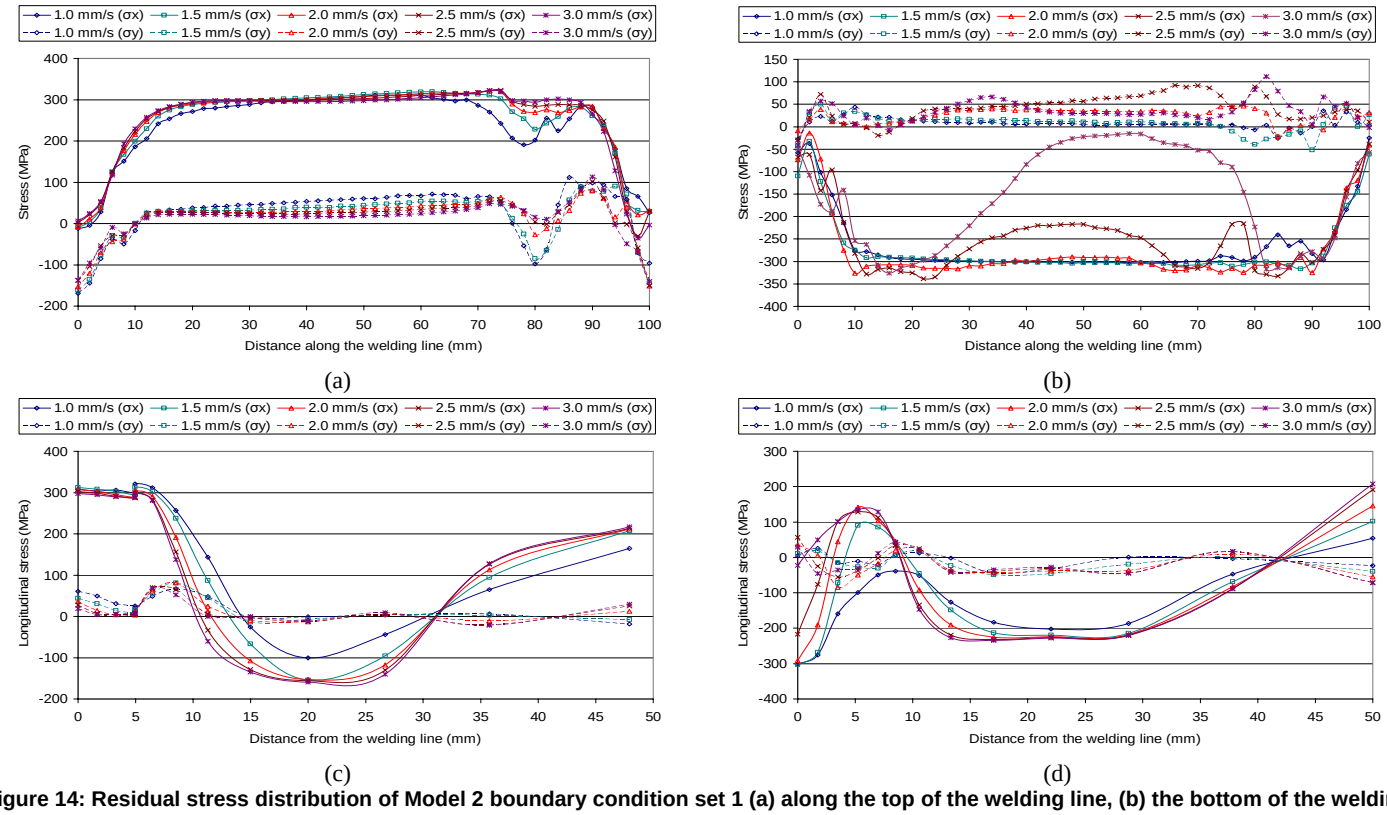

Figure 14: Residual stress distribution of Model 2 boundary condition set 1 (a) along the top of the welding line, (b) the bottom of the welding line, (c) top of the mid-section and (d) bottom of the mid-section for different welding speeds

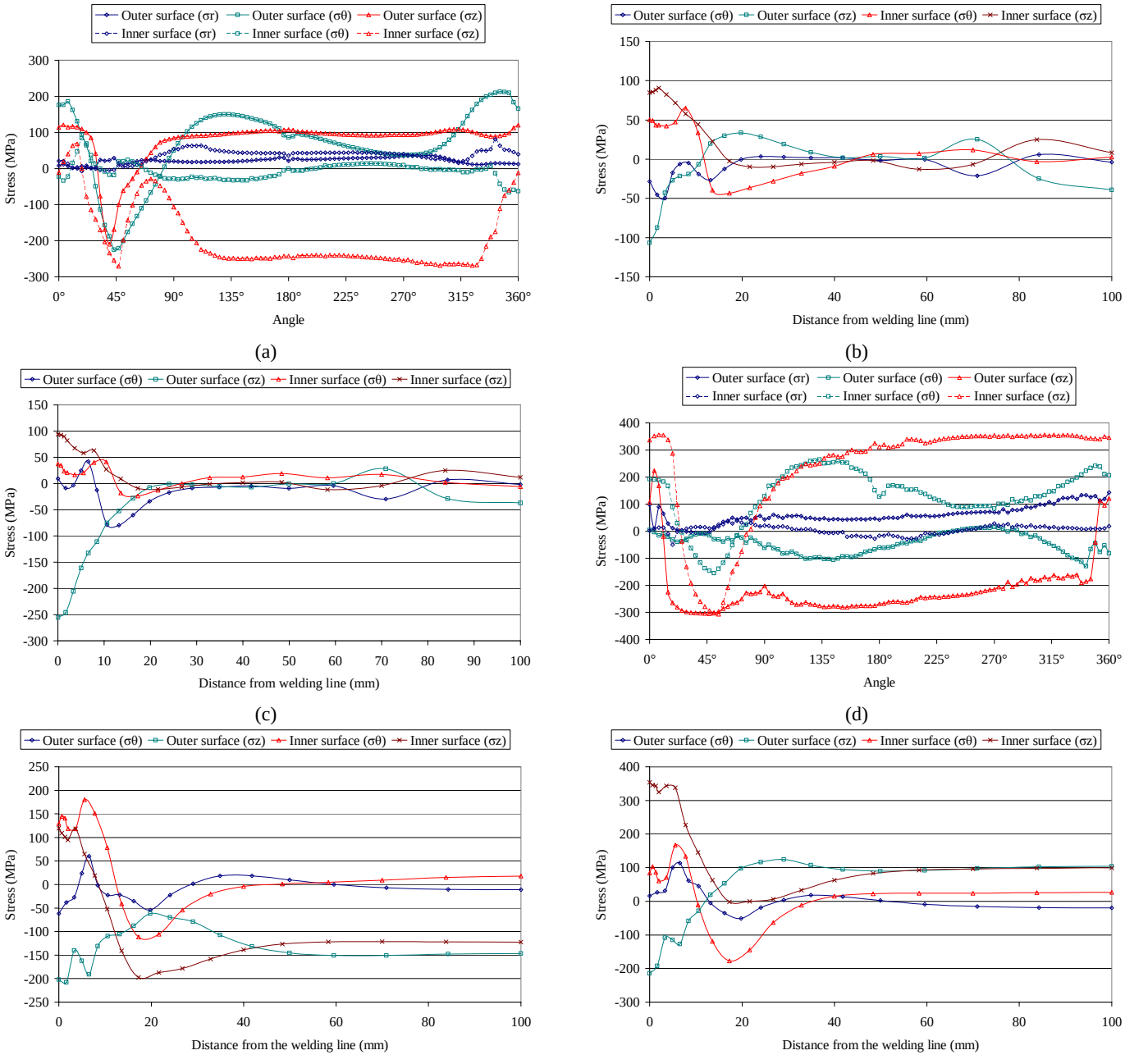

Figure 15: Residual stress distribution in Model 3 (a) along the welding line, (b) the section at 90° and (c) the section at 270° for the fixed structural boundary condition. Residual stress distribution in Model 3 (d) along the welding line, (e) the section at 90° and (f) the section at 270° for the coupled structural boundary condition